Biochemistry

 Volume 42, Number 17 May 6, 2003

Current Topics

Photoactive Yellow Protein: A Prototypic PAS Domain Sensory Protein and Development of a Common Signaling Mechanism†

Michael A. Cusanovich* and Terry E. Meyer

Department of Biochemistry and Molecular Biophysics, University of Arizona, Tucson, Arizona 85721

Received December 6, 2002

Discovery and Properties of PYP. Photoactive Yellow Protein (PYP), originally isolated from an extremely halophilic phototrophic bacterium, has become the structural prototype for the large family of signaling proteins containing the PAS domain amino acid sequence motif. Moreover PYP, as a consequence of its small size, photochemical properties, and the availability of high resolution structural information, has become a key model system in efforts to elucidate the molecular events involved in two-component signaling pathways. In what follows, we will summarize the principal structural and kinetic properties of PYP and explore its relationship to homologous signaling proteins. We are unable to be comprehensive because of space limitations and regret that many references were necessarily omitted. However, related PAS domains, transcriptional regulators with PAS domains, and signal kinase portions of two-component signaling pathways that contain PAS domains will also be explored to determine the extent to which they may show a common mechanism of action in coupling signal-induced conformational changes to domain/domain interactions.

PYP was discovered in *Ectothiorhodospira* (now *Halorhodospira*) *halophila* based upon its color (λ_{max}: 446 nm, ϵ: 45 mM^{-1} cm^{-1}) and its superficial spectral resemblance to 5-deaza-riboflavin-containing proteins (*1*). While attempting to photoreduce the new protein with a laser flash in the presence of flavins and EDTA as a sacrificial electron donor, it was found that it could be reversibly photobleached regardless of the composition of the medium (*2*). At that point, it was realized that it was not a redox protein but had a unique, photoactive chromophore. A misleading attempt was made to change the name of PYP to Xanthopsin, in effect, a yellow-colored opsin (*3*, *4*), but there is no structural similarity whatsoever between soluble PYP and the opsin family of membrane-spanning helical proteins, the rhodopsins of animals and bacteriorhodopsin, halorhodopsin, and sensory rhodopsins of *Halobacterium*, which are in fact related to one another.

PYP is a small soluble cytoplasmic protein (125 residues, 14 kDa) that has a covalently bound *trans-p*-hydroxycinnamic acid (also called *p*-coumaric acid) cysteine 69 thioester as its chromophore (*5*−*8*). The chromophore undergoes trans−cis isomerization during the photocycle, during which the 446 nm absorption maximum is bleached and blue-shifted to about 355 nm within milliseconds and recovers in the dark within 1 s (*2*). The amino acid sequence (*9*), the gene sequence (*4*, *5*), and the three-dimensional structure determined by X-ray diffraction and by NMR (*10*−*12*) all establish PYP as a mixed α/β fold with topology that is now recognized as the structural prototype for a large and diverse family of sensory and signaling proteins that generally contain the PAS sequence motif (acronym based upon period clock protein, aryl hydrocarbon receptor nuclear translocator, and single-minded protein) of approximately 50 N-terminal residues (*13*). The PAS motif is the most conserved segment of PYP and contains many of the active site residues unique to PYP. The C-terminal half of PYP and related proteins corresponds to what is called the PAC motif. The PAC motif is an integral part of the protein, and PAS plus PAC fold as a single structural domain. Henceforth,

† This work was supported in part by a grant from the National Institutes of Health, GM66146.

* Corresponding author. E-mail: Cusanovi@U.Arizona.edu.

10.1021/bi020690e CCC: $25.00
Published on Web 04/09/2003

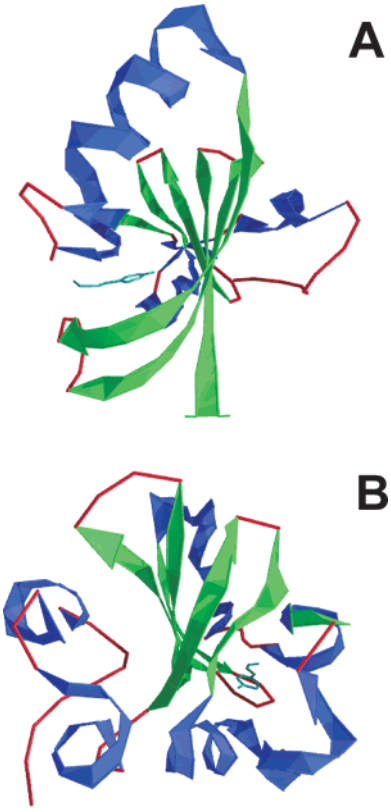

FIGURE 1: Structure of *H. halophila* PYP. Key structural features include the whole PAS domain (amino acid residues 1−125) as opposed to the PAS sequence motif, the N-terminal segment, residues 1−69, which includes the PAS sequence motif, the so-called N-terminal cap or first two helices, the first half of the β-scaffold (strands 1−3), and the chromophore-binding loop with site of covalent attachment to C69. The C-terminal or PAC sequence motif includes the connecting helix and the three C-terminal β-strands 4−6. (A) View with the N-terminal cap at the back, the β-scaffold in the middle (green), the chromophore to the left, and the connecting helix (blue) in the upper left corner. (B) End-on view of the β-scaffold, with the N-terminus on the left, the chromophore to the right, and the connecting helix at the right rear.

when we speak of the PAS (structural) domain as opposed to the PAS sequence motif, we mean the entire protein, PAS plus PAC. A curious observation (*13*) is that BLAST searches with PYP will not identify other PAS domains, but searches with any of the three constituent PAS motifs will identify PYP. This anomaly may be eliminated by substitution of three PYP-specific amino acids, G29F, G47V, and R52Y (*13*). Thus, sequence comparisons alone may not recognize all PAS domains because they are near the limit of detection. Ribbon drawings of the three-dimensional structure, shown in Figure 1, illustrate two views of the PYP fold, which includes a central 6-stranded antiparallel β-sheet flanked by helices. Note the N-terminus with two short helical segments on one side and the chromophore bound to the other side of the central sheet.

H. halophila PYP is quite stable; it requires a midpoint of 7.40 M urea or 2.72−2.75 M guanidine at pH 7 for unfolding as measured by 222 nm ellipticity (*2*, *14*−*16*). When the absorbance at 446 nm is monitored in the dark, it bleaches at nearly the same concentration of denaturant as when monitored at 222 nm. The protein can be boiled for a minute without any permanent damage but has a half-life for irreversible denaturation of approximately 2 h at 90 °C (*2*). When denaturation is monitored by microcalorimetry, the melting temperature is 87 °C but when denaturation is monitored by absorbance at 446 nm, the T_m is 83 °C (*17*). The small difference may be important as discussed below.

Distribution. There are currently seven known species of PYP. In addition to *H. halophila* (Hhal), relatively closely related PYPs have been found in the halophilic purple phototrophic bacteria, *Chromatium* (now *Halochromatium*) *salexigens* (Hsal), and *Rhodospirillum* (now *Rhodothallasium*) *salexigens* (Rsal) (*18*, *19*). PYP from two freshwater species of purple phototrophic bacteria, *Rhodobacter sphaeroides* (Rsph) (*4*, *20*, *21*) and *Rhodobacter capsulatus* (Rcap) (Z. Jiang and C. E. Bauer, 1998, unpublished submission, Genbank accession AF064095 and Integrated Genomics) are not only more divergent in amino acid sequence but show significant differences in spectral properties (two peaks, at 436−446 nm and 360−375 nm) and photocycle (recovery is 100−500-fold faster than Hhal PYP) (*21*, *22*). A hybrid PYP/phytochrome called Ppr was isolated from the thermophilic freshwater purple bacterium, *Rhodospirillum centenum* (now *Rhodocista centenaria*, Rcen Ppr), which differs from other PYPs and phytochromes in that it has binding sites for both *p*-hydroxy-cinnamate and linear tetrapyrrole chromophores (*23*). A Ppr was also recently inferred (*22*) from the genome sequence of the thermophilic purple sulfur bacterium, *Thermochromatium tepidum* (Ttep Ppr) (Integrated Genomics).

Rcen Ppr is the only PYP for which a function is definitely known, as a regulator of transcription of a chalcone synthase homologue (*23*). Chalcone and related compounds are thought to act as sunscreens to protect cells against the harmful effects of UV light. *H. halophila* is negatively phototactic in response to intense blue light with an action spectrum suggestive of PYP (*24*). However, the genome of a closely related species, *Thermochromatium tepidum* (Integrated Genomics) contains a sensory rhodopsin gene associated with those for chemotaxis: CheY, CheW, Htr, and CheA. The Ttep sensory rhodopsin is expected to have a wavelength maximum similar to that of PYP (because of the lack of the color-tuning M118) and may be responsible for negative phototaxis. The *R. capsulatus* genome sequence (Integrated Genomics) shows that the PYP structural and biosynthetic genes are flanked by a cluster of nine to 13 genes for gas vesicle formation and in *R. sphaeroides* (Joint Genome Institute) as many as 14 such genes (*22*), which suggests a role for both Rcap and Rsph PYPs in regulation of cell buoyancy by light. However, none of these speculations have yet been proven.

A BLAST search of more than 70 published genome sequences has not turned up a single PYP beyond those noted above. It is thus likely that PYP is narrowly distributed in phototrophic bacteria as suggested by the Western Blots of Thiemann and Imhoff (*25*) and contrary to those of Hoff et al. (*26*), although there is little doubt that new and unusual species of PYP, that may not cross-react with Hhal antibodies, will eventually be discovered as suggested by the recent reports of PYP from Rsph, Rcap, Rcen, and Ttep.

Sequence and Structure. The amino acid and translated gene sequences of the seven known PYPs (*4*, *5*, *9*, *19*, *20*, *23*; Jiang and Bauer, AF064095) are shown in Figure 2. There are no leader sequences, which is consistent with the cytoplasmic location of PYP and Ppr. Despite the large

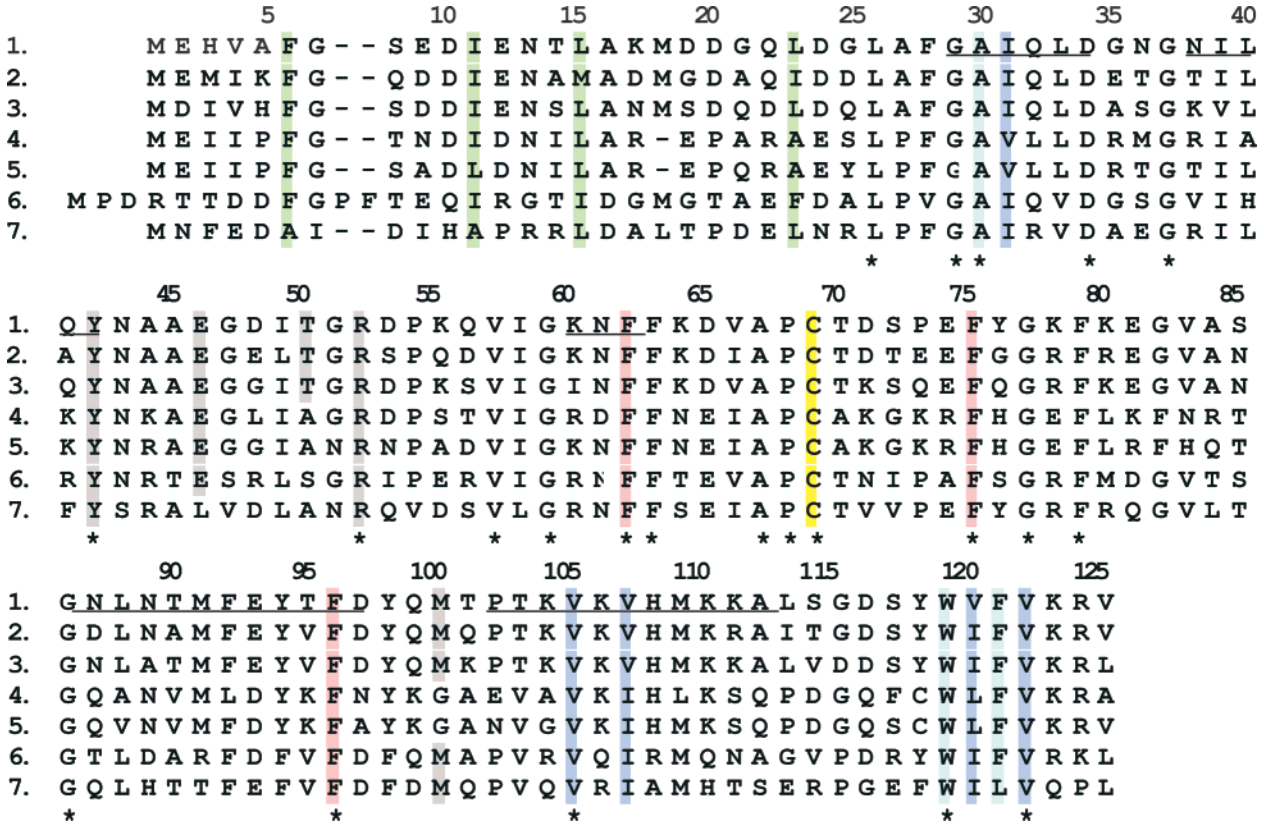

FIGURE 2: Amino acid sequence alignment of known PYPs and related proteins. PYPs from (1) *Hr. halophila*, (2) *Rt. salexigens*, (3) *Hc. salexigens*, (4) *Rb. capsulatus*, (5) *Rb. sphaeroides*, (6) *Rc. centenaria*, and (7) *Tc. tepidum*. The β-scaffold is underlined. The 22 amino acid positions that are absolutely conserved among the known PYPs are indicated with an asterisk. The chromophore binding site, in yellow, is surrounded by hydrophobic residues in red, which interact with hydrophobic residues pointing inward from the β-sheet, in blue. Those residues pointing outward from the β-sheet, in cyan, interact with hydrophobic residues from the N-terminal region, in green. Residues interacting with the chromophore and affecting the photocycle and wavelength maximum are gray.

variation from 30 to 78% identity, there are 22 (18%) absolutely invariant sequence positions in the seven known PYPs, which is high considering the small extent of overall identity. Prominent among these is cysteine 69 that provides the site of binding to the chromophore, colored yellow in Figure 2. The 1.4 Å (*10*) structure of Hhal PYP shows that it adopts an α/β fold centered around a six-stranded antiparallel β-sheet as shown in Figure 1. In Hhal PYP, the E46 (Leu in Ttep) and Y42 side chains hydrogen bond the phenolate oxygen of the chromophore, and the T50 side chain (Ser and Ala in other species) hydrogen bonds the Y42 hydroxyl, colored gray in Figure 2. The substitution of E46 by leucine in Ttep Ppr should result in dramatically different properties if not due to a sequencing error. E46 is situated in a hydrophobic environment surrounded by I31 (Val in other species), I49 (Leu in other species), and invariant V122. This generally hydrophobic environment emphasizes the importance of the hydrophilic interaction of E46 with the chromophore phenolate oxygen and the Y42 hydroxyl. There are two hydrophobic cores located on either side of the central β-sheet in Hhal PYP (*10*) and Rcen Ppr (*27*). The chromophore itself is located in the major core on the inside of the central sheet, surrounded by hydrophobic residues F62, A67, F75, and F96, the most important of which are shown in red in Figures 2 and 3A, all absolutely invariant. These interact with at least five hydrophobic residues from the inside of the central sheet, I31 (Val in others), V105, V107 (Ile in others), V120 (Ile and Leu in others), and V122, shown in blue. In the minor hydrophobic core, at least four hydrophobic residues in the N-terminal 26-residue loop, F6 (Ala in Ttep), I11 (Ala and Leu in other species), L15 (Met or Ile in others), and L23 (Phe, Ile, or Ala in others), green in Figures 2 and 3A, pack against at least three hydrophobic residues from the outside of the central sheet, A30, W119, and F121 (Leu in Ttep) (cyan). The potential significance of the N-terminal loop and the two hydrophobic cores will be described below.

Biosynthesis. The chromophore of PYP is derived from the amino acid tyrosine through deamination and presumably activated for spontaneous binding to apo-PYP through formation of a CoA thioester. In fact, the genes for the biosynthetic enzymes of the chromophore are near the structural gene for PYP (*4*, *28*, *29*; Jiang and Bauer, AF064095). These are tyrosine ammonia lyase (TAL) and *p*-hydroxy-cinnamic acid-CoA ligase (PCL). Recombinant *Rb. capsulatus* TAL was purified and found to be specific for tyrosine (*28*). The activity of the PCL has not yet been characterized. However, a genetic construct, in which all three genes, for PYP, TAL, and PCL, are expressed in *E. coli*, produces holo-PYP (*29*). The biosynthetic enzyme for the phytochrome chromophore in aerobic organisms is heme oxygenase that converts protoheme into biliverdin, which in turn spontaneously reacts with either cysteine or histidine at the active site to form a covalent bond. In plants, the biliverdin is reduced to phycocyanobilin before attachment to the protein (*30*). The heme oxygenase gene is usually

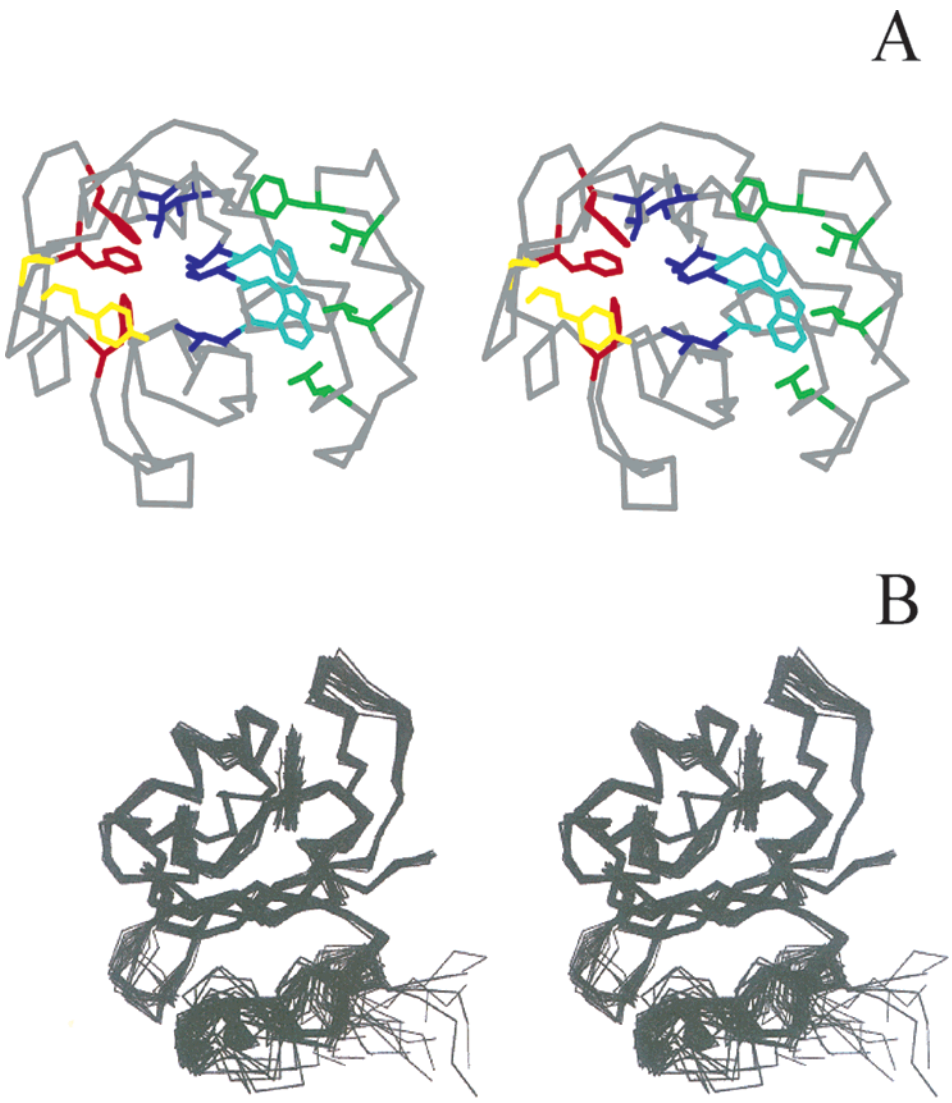

FIGURE 3: (A) Three-dimensional crystal structure of Hhal PYP, in stereo, showing the hydrophobic interactions indicated in the caption to Figure 2, with the same color code, the chromophore on the left, and the N-terminus on the right. (B) NMR solution structure of the ground state Hhal PYP. An ensemble of 26 spectra were used. The relatively disordered N-terminal domain is at the bottom and the chromophore at the top center.

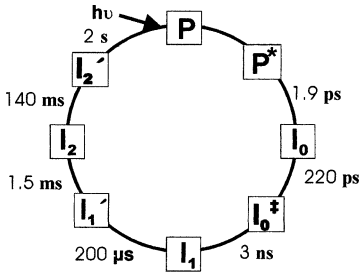

FIGURE 4: Minimal Hhal PYP solution photocycle at room temperature and neutral pH. P is the ground state, an asterisk indicates the excited state, and intermediates (I) are indicated with subscripts and superscripts. Each intermediate is followed by its half-life. Additional intermediates may be present, especially under frozen, crystalline, or dehydrated states.

found immediately upstream of the structural gene for bacteriophytochrome (*31*) but has not yet been identified in *Rc. centenaria* or *Tc. tepidum*.

Dynamic Properties−*Photocycle*. The solution photocycle of Hhal PYP has been determined as shown in Figure 4. Three intermediates were discovered in the initial characterization and called I_1 (210 μs decay), I_2 (4.5 ms decay), and I_3 (625 ms decay) (*2*), but in a subsequent publication, the small amplitude, second-phase bleach reaction from I_2 to I_3 was no longer observed, and the fully bleached intermediate I_3 was relabeled I_2 (now 133 μs formation and 385 ms decay) (*32*). The nomenclature of intermediates then remained stable for about seven years, although rate constants were found to change with conditions of the experiment. However, other workers relabeled the I_1 intermediate, pR or PYP_L, and the more recently designated I_2 intermediate, pB or PYP_M, for no apparent reason (*3*, *33*, *34*). The small amplitude second-phase bleach was rediscovered (*35*−*38*) and ascribed to I_1', I_2', or pB′ (1.2−2 ms decay). We have adopted the convention that I_2 is structurally the furthest intermediate from the ground state before recovery, although others see I_2 as the first protonated intermediate. Because the 1−4 ms kinetics correspond to a bleach, the proper designation should be I_1'. A simultaneous flip of the chromaphore into solvent and proton transfer (M. Heyn, personal communication) occurs in the faster bleach phase (I_1 to I_1'), and a conformational change of the protein occurs in the slower phase (I_1' to I_2). Biphasic (150−600 ms and

0.58−2.0 s) decay of I_2 to ground state was also observed (*35*, *37*, *38*) with formation of a new intermediate, which should be designated I_2'. Both proton transfer and conformational changes should occur during the large amplitude decay of I_2 to I_2', but it is unclear what occurs during the small amplitude I_2' to ground-state transition. The rise time of I_1 was shown to be 3 ns by picosecond spectroscopy, and two new intermediates were discovered, I_o and $I_o^{\ddagger}$ (*39*). I_o and $I_o^{\ddagger}$ have similar red-shifted spectra with maxima near 510 nm but with differing amplitudes and are formed in about 3 and 220 ps. Using higher resolution femtosecond spectroscopy, the actual lifetime of the excited state was shown to be 1.9−3.6 ps (*40*, *41*). The quantum yield for the formation of I_2, presumably the signaling state, is 0.64 (*32*) or 0.35 (*42*). The quantum yield for fluorescence, on the other hand, is very small, 0.0014−0.0035 (*43*, *44*).

Crystalline PYP was shown to undergo a different photocycle in that decay of I_2 was distinctly biphasic), whereas the same protein in solution appeared to be monophasic (*45*). At low temperature, PYP also undergoes a somewhat different photocycle with formation of both blue- and red-shifted species at 430 and 490 nm (*44*). This work was repeated with gradual warming of the frozen, irradiated sample to produce additional low-temperature intermediates, presumably involved in parallel pathways (*46*). These low-temperature intermediates were called PYP_B (489 nm), PYP_H (442 nm), PYP_{BL} (400 nm), PYP_{HL} (447 nm), and PYP_L (456 nm). Some of these intermediates may be similar to those observed at room temperature (*34*), but no direct correspondence has been established, and they should not be equated. It is thus fitting that they should be named differently. Dried samples of PYP also have an abnormal photocycle (unpublished results). In all three cases where PYP is restrained, whether in crystals, the frozen state, or dehydrated, the properties are significantly different, suggesting that dynamics or conformational changes are important.

The solution photocycle bleach and recovery are strongly affected by alcohols and by viscosity, consistent with a protein conformational change that exposes a hydrophobic region to solvent (*32*). A change in heat capacity (*47*, *48*) inferred from curved Arrhenius plots for recovery of photobleached PYP as a function of temperature (*32*) also indicates that a hydrophobic region is exposed to solvent during the photocycle. The photobleached I_2 state binds to lipid bilayers (*49*) and to dyes (*38*), consistent with transient exposure of a hydrophobic site.

The PYP solution photocycle is not strongly affected by ionic strength or by cations or anions in general (*2*). However, it is now known that ions of the chaotropic and kosmotropic series have a pronounced effect on the absorption spectra (*50*). There is also a marked dependence on pH for both bleach and recovery (*51*), which appears to reflect strongly altered pK_a values for E46 and the chromophore hydroxyl in the folded protein and when exposed to solvent following flash photolysis. A quantitative analysis of the unusual protonation states of the chromophore and E46 indicate that electrostatic interactions in the low dielectric protein interior cause a reversal of the relative pK_a values from what they are in a high dielectric medium (i.e., E46 in the folded protein has a pK_a approximately equal to that for alkaline denaturation, which is near 11, and the chromophore hydroxyl has a pK_a equal to that for acid denaturation of the protein, which is about 2.7 (*52*)). There is a net uptake of one proton upon bleaching at acidic pH and subsequent release upon recovery (*53*). At neutral pH, there is no net proton uptake, and at alkaline pH, there is a net release followed by uptake on return to the dark state (*54*). Again, this reflects changing pK_a values for E46 and chromophore during the photocycle. Using FTIR to follow changes in the protonation state of E46, it was concluded that the proton is transferred directly from E46 to the chromophore during progression of the photocycle and that this proton-transfer triggers a conformational change leading to the signaling state (*36*, *55*, *56*). It has been confirmed that proton uptake kinetics are synchronized with the fast phase of I_2 formation (I_1 to I_1') (*35*, *38*). However, the E46Q mutant, which cannot transfer a proton from glutamine to chromophore, has kinetics for the formation of I_2 that are accelerated relative to wild type but remain coupled to proton uptake (*35*, *38*). Thus, proton transfer, from E46, does not trigger the conformational change nor is it rate-limiting in formation of I_2.

Crystallographic Structure of Intermediates. In one of the first demonstrations of the power of time-resolved Laue crystallography, the structure of a long-lived intermediate, thought to be equivalent to the signaling state I_2, was determined (*57*). When the chromophore isomerizes, the hydrogen bonds to E46 and Y42 are broken, and the chromophore becomes exposed to solvent. To accommodate the cis conformation of the chromophore, R52 swings out of the way and forms a new hydrogen bond with the phenolic oxygen. The photobleached and dark state structures in the region of the chromophore are compared in Figure 5. These same changes are likely to occur in solution, but there could be additional, more dynamic, changes not allowed by crystal constraints as will be discussed below.

The extension of time-resolved crystallography to nanosecond resolution allowed determination of the structure of an earlier intermediate, presumably equivalent to I_1 (*58*). In this structure, the chromophore is fully in the cis conformation, but the center of the aromatic ring is unmoved; it has lost its hydrogen bond with E46 but retains that to Y42. The time-resolved crystallography also resulted in a nanosecond to second molecular movie of the photocycle from which two new, spectroscopically silent, intermediates are proposed with half-lives of 33 ns and 2.5 μs (*59*). In addition, the interpretation of the electron density of the earlier study (*58*) was revised to incorporate the entire time frame. The photocycle of the crystalline state is now seen to be initiated by a flip of the thioester carbonyl (*60*) as first proposed in (*55*), which persists until the protein enters the I_2 state. Unfortunately, the molecular movie does not conclude with testable detailed structural models for the crystalline intermediates, which have now reached six in number.

A cryo-trapped early intermediate at much higher, 0.85 Å, resolution (*60*) shows a similar electron density map as for the 1 ns time-resolved crystal (*58*), but it was interpreted very differently. In this structure, presumably for the low-temperature intermediate, PYP_{BL}, the chromophore isomerizes by rotating the thioester linkage with the protein (166° degrees relative to the plane of the aromatic ring), which results in a distorted transition-state-like conformation in which the double bond is neither cis nor trans but trapped between (with a torsion angle of −80°). Significantly, the

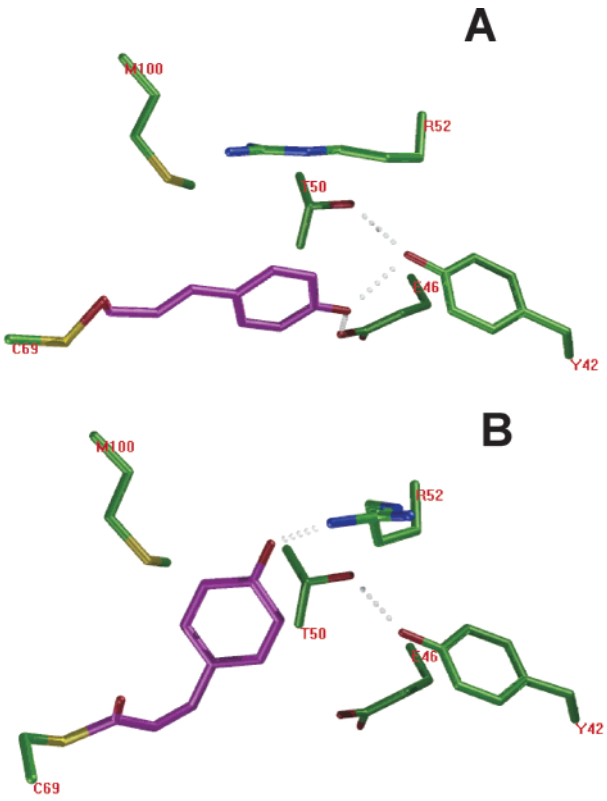

FIGURE 5: PYP protein−chromophore interactions known to affect the absorption spectra and solution photocycle. (A) Ground-state trans chromophore (magenta) where dotted lines represent probable hydrogen bonds to amino acid side chains (green). (B) Phototobleached I_2 or cis chromophore (presumed signaling state).

hydrogen bond to E46 is retained in this structure as shown by FTIR (*35*, *36*, *55*, *61*) and in contrast to the crystallographic structure of I_1 (*58*) where it appears to be broken.

NMR Solution Structure. When dealing with a sensory protein that is expected to change conformation in the signaling state, crystal structures may not provide the complete picture. Thus, NMR solution structures are expected to complement the crystallographic data. The principal difference in the ground-state solution and crystallographic structures of PYP is in residues 19−23, which adopt a helical conformation in the crystal structure but are somewhat disordered in the solution structure (*11*). In addition, residues 1−5 and 113−118 show substantial mobility in the solution structure. Although they cannot be directly equated, the crystallographic temperature factors are also high for these regions of the structure (*10*) consistent with agreement in the two approaches. By way of contrast, the long-lived I_2 intermediate shows considerable disorder in the solution structure, primarily in the N-terminal helical region but extending throughout the structure to strands I and VI of the central sheet and to the chromophore-containing loop (*62*). Figure 3B shows an ensemble of the NMR solution structures of ground-state Hhal PYP and illustrates the dynamic regions. This disorder was not apparent in the ground-state crystal structure nor of the I_2 intermediate where changes were localized to the immediate vicinity of the chromophore (*57*). Disorder in itself cannot fully explain the nature of the signaling state but suggests that the N-terminus may move with respect to the rest of the protein to allow a new hydrophobic interaction with a reaction partner receptor protein in the bleached I_2 state. The relatively small changes in the crystal structure of I_2 do not explain the exposure of a hydrophobic site during the photocycle (*32*) or the much lower stability of I_2 (1.75 vs 2.72 M guanidine denaturant for ground state) and the more than 19% loss of 222 nm ellipticity during photoexcitation (*15*, *16*, *63*). An internal water, that connects G7 to H108 via a hydrogen bond, is exposed to solvent in the I_2 state and that interaction is lost in the H108F mutant (*64*). These data support a model in which structural changes at the chromophore in the I_2 state are transmitted to the N-terminus, which is bound to the remainder of the protein through hydrophobic contacts in the ground state (*10*). The hydrophobic residues connecting the chromophore to the N-terminus are illustrated in Figure 3A. If the N-terminus were to swing away from the central β-sheet, the exposed hydrophobic side chains could conceivably cause the helical segments to rearrange, resulting in the partial loss of ellipticity observed for I_2, in the decrease in stability to denaturation, and in the disorder at the N-terminus.

PYP Mutants. The amino acid residues in PYP that have been identified from crystallography as most likely to affect the properties of the chromophore are Y42, E46, T50, R52, and M100 (see Figure 5). Single site mutations Y42F, Y42A, E46Q, E46A, E46D, T50V, T50A, R52A, R52Q, M100A, M100L, M100K, and M100E have been constructed and at least partially characterized (*17*, *33*, *50*, *51*, *65*−*68*). The major effects of mutations at Y42 are on the spectral properties and stability with lesser effects on kinetics of the photocycle where formation of I_2 is twice as fast in Y42F, recovery is half that of wild type (*50*), the lifetime of the excited state has doubled, and formation of I_1 is 100 times faster than wild type, most likely because of the loss of the Y42 hydrogen bond (*69*). In the absorption spectrum of the ground state of Y42F, an intermediate absorption peak appears on the short wavelength side of the 458 nm maximum in the vicinity of 390 nm (*65*), and chaotropes, kosmotropes, and temperature have strong effects on the relative amplitude and wavelength maxima (*50*). It appears that the wild-type protein and virtually all mutants tested, except those containing substitutions at E46, are capable of forming the intermediate spectral form with a wavelength maximum between 370 and 390 nm (*17*). A reasonable model for the intermediate spectral form is a change in the E46−chromophore hydrogen bond strength either through changes in geometry and/or in hydration and alteration of the dielectric environment (*50*).

The major effect of mutant E46Q is on photocycle kinetics in which both formation and recovery of the I_2 intermediate are dramatically accelerated with increasing pH in contrast to wild type, where the formation of I_2 is slowed with pH and recovery shows a bell-shaped dependence described by two pK_a values (*51*). It is likely that the E46Q pK_a of 8.0 for recovery is due to ionization of the chromophore (*17*). The pK_a for ionization of the chromophore in the folded protein is increased significantly in E46Q (from 2.7 to 5.0) and even more so in E46A (to 7.9) and E46D (to 8.6), which approach that of the chromophore in solution (about 9.0) (*67*). The first intermediate I_o is formed more slowly in E46Q at pH 7 (3 ps as compared with 1.9 ps), but subsequent steps are faster ($I_o^{\ddagger}$ 8 ps instead of 220 ps, and I_1 0.7 ns instead of 3 ns) (*41*, *70*). This was ascribed to the weaker amide to

chromophore hydrogen bond. For mutant E46A at pH 9.5, where the chromophore is ionized, the formation of I_o is 5.3 ps and of I_1 is 40 ps (no $I_o^‡$ was observed) (*69*). The more rapid formation of I_1 was ascribed to one less hydrogen bond to the chromophore, permitting more facile rearrangement. The absense of E46 in Ttep Ppr should result in properties similar to the Hhal E46A mutant.

Mutants T50V and R52A show small redshifts in the absorption spectrum and have minimal effects on the photocycle kinetics (*50*, *51*). T50 normally hydrogen bonds Y42 in wild-type protein (Figure 5) but directly hydrogen-bonds to the chromophore in the Y42F mutant (*10*, *50*). The double mutant Y42F/T50V has a greater proportion of the 390 nm intermediate form than does the Y42F mutant (*17*). Thus, Y42 and T50 stabilize the chromophore in the 446 nm form. Nevertheless, the minimal effects of mutation at T50 combined with observation of naturally occurring substitutions at this position indicate that it is less important than Y42 and the other active site residues. The negative charge on the chromophore was postulated to be partially stabilized by the nearby positive charge on R52 (*3*, *10*), but the minimal effects of mutation suggest that this is not the case.

Mutations M100A, M100L, and M100K have dramatic effects and M100E a lesser effect in slowing recovery of the photocycle by as much as 3 orders of magnitude such that room light is sufficient to produce a steady-state bleach (*66*, *68*, *71*). It has been shown with wild type and more directly with the M100A I_2 intermediate that recovery can be accelerated by 6 orders of magnitude over dark recovery and 3 orders of magnitude faster than wild-type dark recovery by excitation with 365 nm light (*66*, *72*, *73*). The more rapid photoreversal versus dark recovery suggests that cis−trans isomerization of the chromophore could be catalyzed by the M100 sulfur (*66*). Dark recovery in M100A is nearly as fast as in wild type at high pH, suggesting that the anionic form of the chromophore isomerizes more readily than does the neutral form. The crystal structure of the Rcen PYP domain indicates that the loop containing residues 97−100 adopts a different conformation that limits access of M100 but increases solvent access to the chromophore (*27*). This may partially explain the more than 300-fold slower recovery in Ppr (*23*). Rsph and Rcap PYPs have naturally occurring M100G substitutions; thus, it is unclear why recovery in Rsph PYP is accelerated relative to wild type Hhal PYP by 100-fold (*21*).

The NMR solution structure indicates large disorder of the N-terminus of the protein in the I_2 intermediate (*62*); thus, it was postulated that the N-terminal loop swings out in the signaling state. However, mutations G47S, G51S, and G47S/G51S that could serve as a hinge for the conformational change had minimal effect on kinetics (*74*). Deletion of the N-terminal 6, 15, or 23 residues had much the same effect as M100 mutants in dramatically slowing recovery by 140−4500-fold (*75*). Similarly, slow recovery was observed when 25−27 residues were deleted from the N-terminus (*76*). It is unlikely that a protein having such massive deletions would be stable enough to fold unless the N-terminus is only weakly associated with the remainder of the protein or folds as a separate domain. That there is no observed natural variation in the length of the PYP N-terminus, except for a single-residue deletion in Rsph and Rcap, indicates that the N-terminus is an important region of the protein.

PYP as a Prototypic Structure for the PAS Domain Sequence Motif. The PAS domain family contains diverse sensory proteins that generally share an amino acid sequence motif, and based upon BLAST searches, PYP was identified as a PAS sequence homologue (*77*, *78*). PAS domains are near the limit of detection by sequence comparisons alone, but it is well-known that the three-dimensional structure is more highly conserved than is amino acid sequence and that is the basis we have adopted to identify homologous PAS domains in this review. The PYP three-dimensional structure was one of the first to be determined for this family of proteins (*10*) and serves as the prototype for all. The three-dimensional structures of the N-terminal domain of the oxygen-binding heme protein FixL (*79*−*81*), the N-terminal domain of the voltage-regulated potassium channel protein HERG (*82*), the yeast YKG9 protein, (*83*), the FMN-binding LOV2 domain of a phototropin homologue (*84*), the pheromone-binding domain of the quorum-sensing protein, TraR (*85*, *86*), the PAS domain of a mouse membrane-trafficking protein, Sec22b (*87*), the cyclic-GMP-binding GAF domain of phosphodiesterase 2A, PDE2 (*88*), and the phosphatidyl inositol- and actin-binding profilin (*89*) establish them as structural homologues of the prototypic PYP. Several homologues of PYP are illustrated in Figure 6 where the structures of HERG, LOV2, PDE2, and FixL are overlaid on that of PYP, and in Figure 7 the structures of the TraR/DNA complex, Sec22b, YKG9, and the profilin/actin complex are shown. The amino acid sequences were aligned based upon the three-dimensional structures as shown in Figure 8 where secondary structure is also indicated. The central β-sheet is conserved as β1-β6, although the length and number of individual strands varies. α-Helices α1 and α2 are conserved in the *Sinorhizobium* FixL construct, and N-terminal helices are found in YKG9, TraR, and Profilin. Helices α3 and α4 are present in most structures but are absent in YKG9 and TraR. Helix α5 is completely conserved. There is no C-terminal helix in PYP, but there is in the *Bradyrhizobium* FixL construct, LOV2, YKG9, and profilin. Based upon secondary structure predictions for the holo-FixL and holo-LOV2 proteins, they are likely to have both N- and C-terminal helices that were unintentionally truncated in the constructs used for structure determination, but which are likely to interact with one another as in YKG9 and may have functional importance (see below). Models based on PYP and FixL were constructed for the aryl hydrocarbon receptor (*13*, *90*), but the structure has not yet been determined. The importance of the PAS domain family is shown by its presence in most forms of life (plants, animals, and bacteria) (*78*). There are as many as 140 and 87 different PAS and GAF domains identified in *Anabaena* alone (*91*), and many hundreds have been identified in genomes sequenced to date (*92*). Furthermore, the tetrapyrrole-binding domain in phytochrome appears to be related to the cyclic nucleotide-binding GAF domain (*93*). Given the variety of ligands that have been found to bind to PAS domains and the protein modifications necessary to accommodate those ligands, a uniform nomenclature should be developed. We propose to name the PAS domains according to the type of ligand, thus, Heme-PAS, abbreviated H-PAS, Flavin (F-PAS), *p*-hydroxy-cinnamate (C-PAS), Quorum-(Q-PAS),

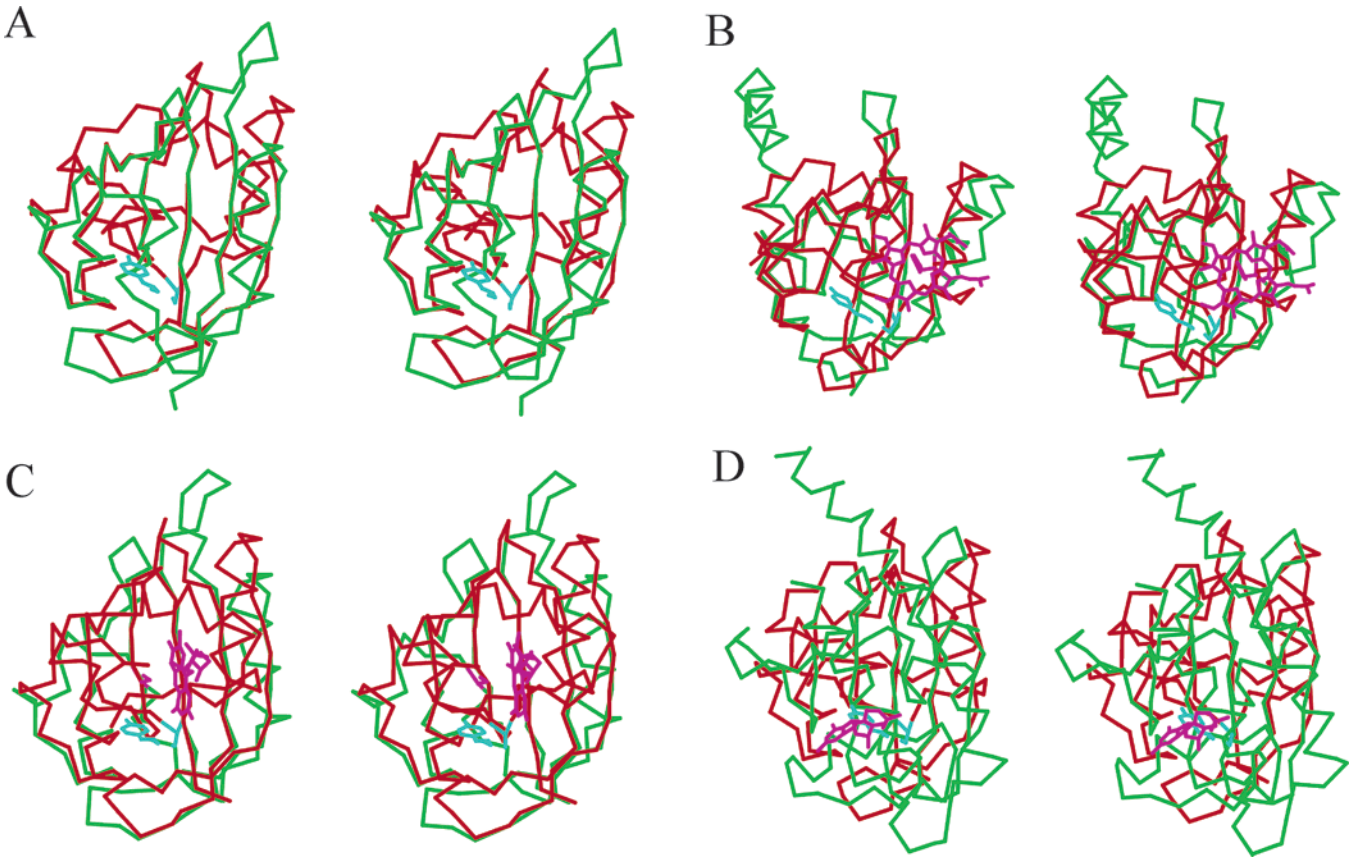

FIGURE 6: Stereo backbone overlays of the PAS domains that are most similar to PYP, all in approximately the same orientation. (A) PYP (red)—HERG (green), the PYP *p*-hydroxy-cinnamic acid chromophore (cyan). (B) PYP (red)—SM FixL (green), heme (magenta). (C) PYP (red)—LOV2 (green), FMN (magenta). (D) PYP (red)—PDE2 or GAF (green), cyclic GMP (magenta).

phosphatidyl-inositol (I-PAS), cyclic GMP (G-PAS), and linear tetrapyrrole (T-PAS).

The heme in FixL (*79*, *81*), the flavin in LOV (*84*), the cyclic GMP in GAF (*88*), and the 3-oxo-octanoate-homoserine lactone in TraR (*85*, *86*) are bound to approximately the same region of the protein as the *p*-hydroxy-cinnamate in PYP (i.e., on the same side of the central β-sheet). The changes in the crystal structure induced by oxygen-binding in FixL are minimal (*79*, *80*), just as they are upon photoactivation in LOV2 (*84*) and in PYP (*57*). This does not preclude significant structural changes in solution, as seen for PYP.

It is interesting that the disordered 25-residue N-terminus of the HERG PAS domain is essential for its function and that the recombinant PAS domain has been shown to bind to potassium channels in which the PAS domain has been deleted (*82*). Deletion of 23−26 residues at the N-terminus of the HERG PAS domain has the same effect as deletion of the entire PAS domain, whereas deletion of the first nine residues has a smaller effect similar to F29A and Y43A mutations in the central β-sheet (*82*). The central sheet in the HERG PAS domain forms a hydrophobic dimerization patch in the crystal structure that may provide the interface through which it binds to the remainder of the potassium channel.

The N-terminus of FixL is disordered in the crystal structure of the *Bradyrhizobium* protein (*79*), which may require the longer N-terminus that is present in the *Sinorhizobium* FixL (*81*) for proper folding through N- and C-terminal interaction as seen with other PAS domains in Figures 6 and 7. In all three engineered proteins, FixL, Lov2, and HERG, important segments at both the N- and the C-termini may have been inadvertently deleted as compared with the structures of the holoproteins YKG9, TraR, and profilin. As discussed above, the N-terminus of PYP packs against the central β-sheet through hydrophobic interactions and appears to be disordered in the bleached state (*10*, *62*). Furthermore, PYP denatures at two temperatures, where color is lost at 83 °C and the protein completely unfolds at 87 °C (*17*) as noted earlier. Thus, a case may be made for the N- and C-termini plus the hyrophobic residues in the central β-sheet in all of the PAS domain-containing proteins to play a significant role in formation of the signaling state and in the interaction with receptor. This can be seen in TraR, where both N- and C-terminal helices are involved in formation of the functional dimer and in interaction with the DNA-binding domain when the ligand is bound (*85*, *86*) as shown in Figure 7B. Actin binds to the C-terminal helix and a portion of the β-sheet of profilin when there is no ligand (*89*). The ligand-binding site of profilin is unknown, but there is a basic patch composed of residues K37, K69, K90, and K115 near the ligand-binding site of the other PAS domains on the opposite side of the β-sheet from the actin-binding site that could provide an electrostatic binding site for inositol phosphate, the headgroup of phosphatidyl inositol, and the profilin ligand. Thus, the ligand-binding sites of the PAS domains are on one side of the β-sheet, and the protein-binding sites, where they have been determined, are on the other side of the β-sheet near the N- and C-terminal helices.

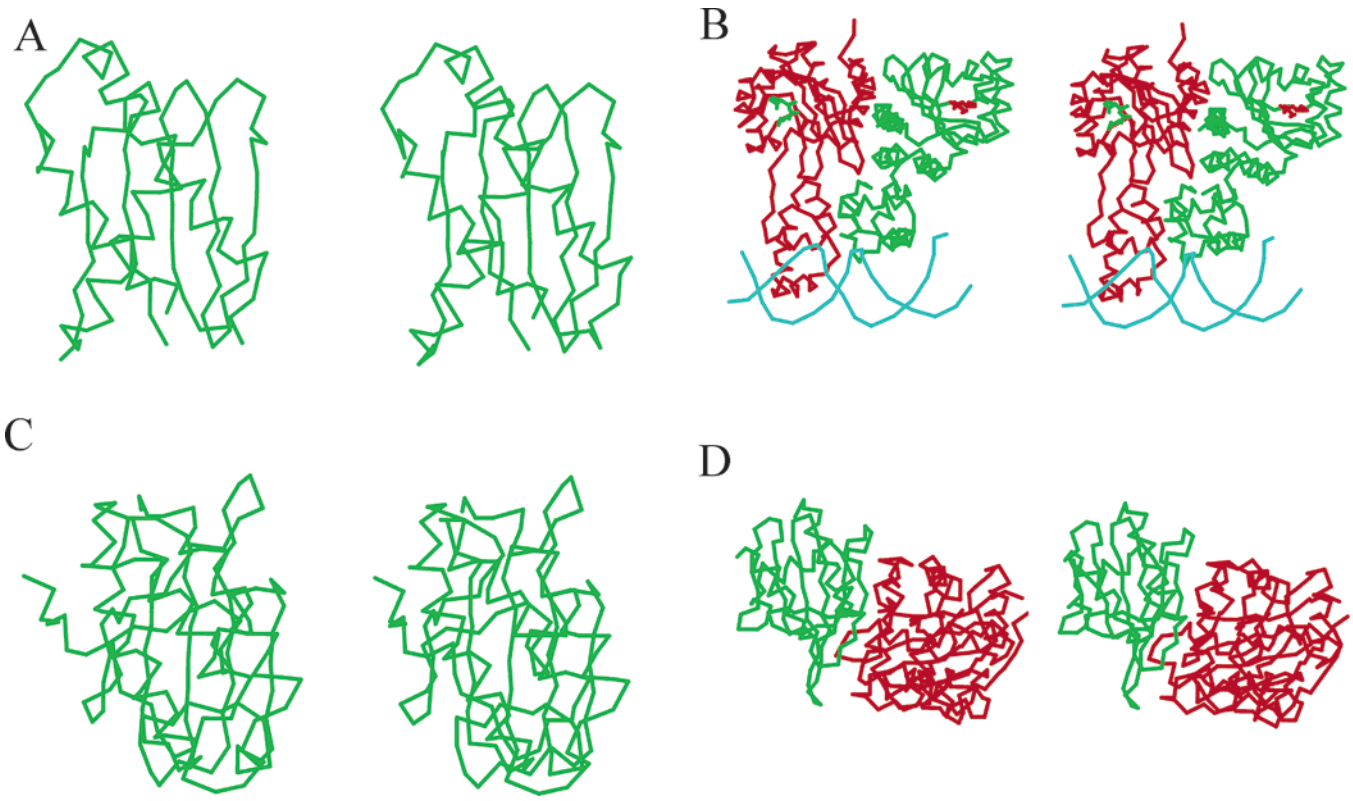

FIGURE 7: Stereo representation of the more divergent PAS domains. (A) Mouse Sec22b (no ligand). (B) Dimeric TraR (red and green)−DNA (cyan) complex with bound homoserine lactone ligand (green and red). (C) Yeast YKG9 (no ligand). (D) Profilin (green)−Actin (red) complex (no ligand). Panels A, C, and D are in the same orientation as the four structures in Figure 6. The axis of the DNA in panel B is approximately aligned with the plane of the page.

Development of a Common Signaling Mechanism. It has been suggested that the N-terminus of PYP might be involved in signaling via N-terminal disorder induced by photoactivation of the chromophore, breakage of the E46/chromophore hydrogen bond, loss of the E46/G29 interaction, and perturbation of the adjacent F28, which interacts with the N-terminus (*94*). We believe that there may be a common signaling mechanism for the majority of PAS domains whereby the signal is transmitted from the ligand-binding site and associated hydrophobic residues in contact with the ligand through distortion of the central β-sheet to the interacting N- and C-termini (that are involved in protein/protein contacts) and their associated hydrophobic residues. Expanding and modifying the Craven et al. (*94*) mechanism, it is plausible that in the case of PYP, photoisomerization of the chromophore (on one side of the central sheet in Figure 1A) and exposure to solvent leaves behind a hydrophobic cavity including F62, F75, and F96, red in Figures 2 and 3A, which collapses upon itself, thus resulting in distortion of the residues on the chromophore side of the central β-sheet, I31, V105, V107, V120, and V122 (blue), and the interaction of hydrophobic residues on the opposite side of the sheet, A30, W119, and F121 (cyan), which hold the N-terminal helices in place through hydrophobic interaction with F6, I11, L15, and L23 (green). In contrast to the Craven et al. (*94*) mechanism, the hydrophobic collapse model suggests that E46 and G29 are less important than the more extensive hydrophobic interactions. In each of the PAS domain-containing proteins, a similar mechanism involving communication among ligand, central β-sheet, and the N- and C-terminal helices may be operative as much through steric interactions as by hydrophobic contacts. In FixL, oxygen binding to the heme may result in steric hindrance, which may cause distortion of the central β-sheet and may alter its interaction with N- and C-terminal helices. In Lov, formation of the C38-C4A adduct of the flavin may likewise cause distortion of the β-sheet through collapse similar to that in PYP. In profilin, ligand binding disrupts the interaction with actin. On the other hand, ligand binding in TraR may stabilize the protein and promote interaction between the β-sheet and the N- and C-termini. The common elements of the proposed mechanism are alteration of the ligand-binding site through environmental sensing, distortion of the central sheet caused by altered interactions at the ligand-binding site, and either weakening or strengthening the interaction of the N- and C-terminal helices with the central β-sheet and with interacting proteins or domains.

Key Questions Relating to Signal Transduction. Central issues include a more detailed understanding of the molecular events leading to the signaling state, developing a better understanding of the role of the N- and C-terminal domains in signal transduction, understanding the interaction of PAS domains with their binding partners (often a response regulator), and characterization of the regulation and expression of PAS domain-containing signaling proteins. Finally, there is considerable interest in obtaining information on the ligands and/or sensing mechanism for a broader group of PAS domain-containing proteins, for example HERG and YKG9. Given the very large number of PAS domain-containing proteins identified in genomes, there is no doubt that many new PAS ligands and two-component signaling pathways containing PAS domains will be described in the future. In this context, it seems likely that the insights derived from the characterization of PYP will be of significant value

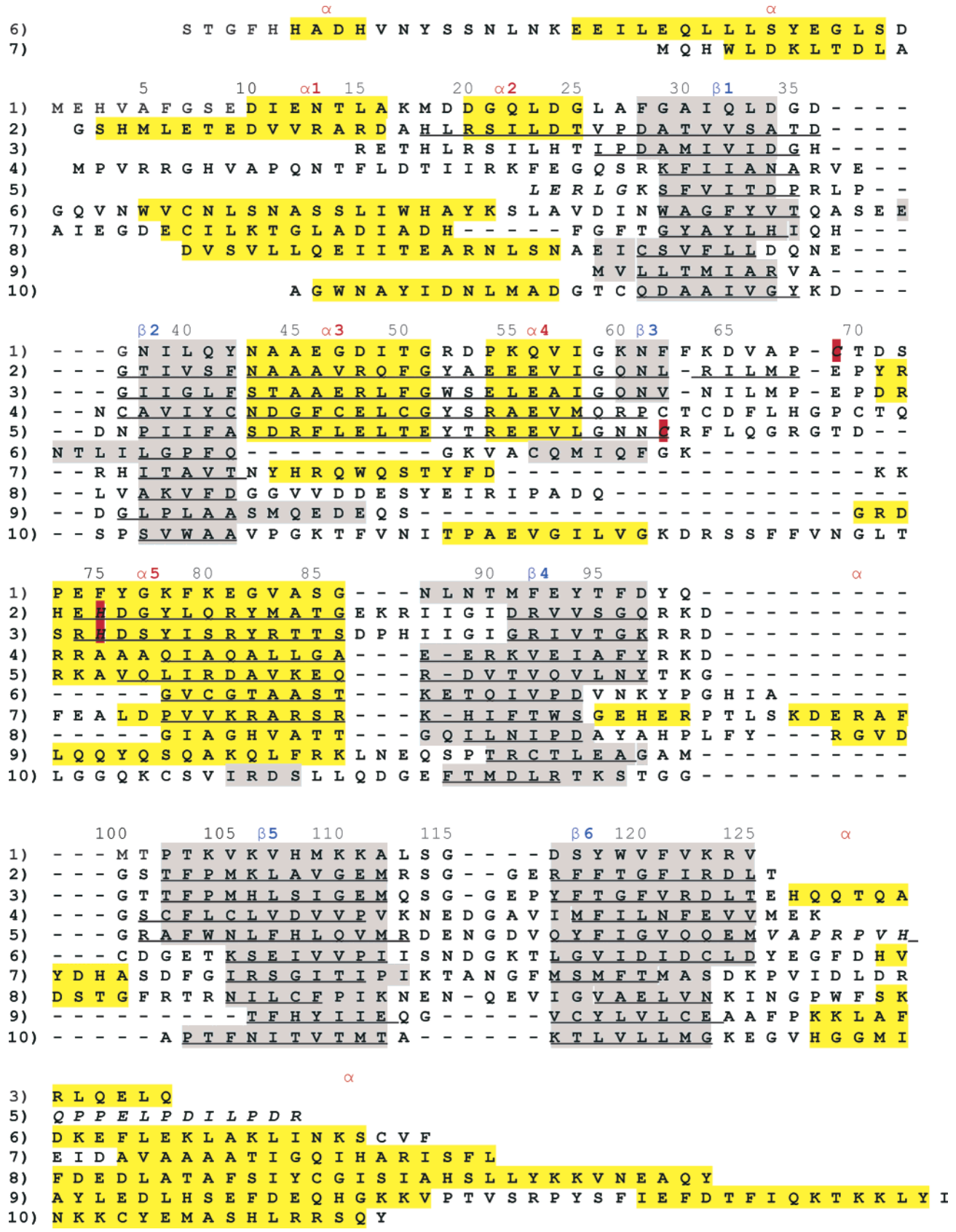

FIGURE 8: Amino acid sequence alignment of PAS domain-containing proteins according to the three-dimensional structures and using the PYP numbering throughout. (1) Hhal PYP holoprotein with chromophore-binding C69 (red). (2) Engineered *S. meliloti* FixL heme domain with heme-binding His 75 (red). (3) Engineered *B. japonicum* FixL heme domain. (4) Engineered N-terminal human voltage-gated potassium channel regulatory domain (HERG). (5) Engineered fern Phy3 LOV2 FMN-binding domain with reactive C62 (red). (6) Yeast YKG9 holoprotein. (7) TraR Quorum-sensing transcriptional regulator, N-terminal domain. (8) Engineered mouse Sec22b PAS domain. (9) Mouse phosphodiesterase PDE2 GAF domain. (10) Bovine profilin holoprotein. Gray—β-sheet, yellow—α-helix, underlined—structurally similar to PYP, and italics—disordered regions in crystal structures. Secondary structure is numbered according to the PYP fold. Extra segments, not present in PYP, are not numbered.

in understanding and manipulating the mechanisms and biological activities of a wide range of signaling proteins.

REFERENCES

1. Meyer, T. E. (1985) *Biochim. Biophys. Acta 806*, 175−183.
2. Meyer, T. E., Yakali, E., Cusanovich, M. A., and Tollin, G. (1987) *Biochem. 26*, 418−423.
3. Hellingwerf, K. J., Hoff, W. D., and Crielaard, W. (1996) *Mol. Micro. 21*, 683−693.
4. Kort, R., Hoff, W. D., Van West, M., Kroon, A. R., Hoffer, S. M., Vlieg, K. H., Crielaard, W., Van Beeumen, J. J., and Hellingwerf, K. J. (1996) *EMBO J. 15*, 3209−3218.
5. Baca, M., Borgstahl, G. E. O., Boissinot, M., Burke, P. M., Williams, D. R., Slater, K. A., and Getzoff, E. D. (1994) *Biochemistry 33*, 14369−14377.
6. Hoff, W. D., Düx, P., Hård, K., Devreese, B., Nugteren-Roodzant, I. M., Crielaard, W., Boelens, R., Kaptein, R., Van Beeumen, J. J., and Hellingwerf, K. J. (1994) *Biochemistry 33*, 13959−13962.
7. Hoff, W. D., Devreese, B., Fokkens, R., Nugteren-Roodzant, I. M., Van Beeumen, J. J., Nibbering, N., and Hellingwerf, K. J. (1996) *Biochemistry 35*, 1274−1281.
8. Imamoto, Y., Ito, T., Kataoka, M., and Tokunaga, F. (1995) *FEBS Lett. 374*, 157−160.
9. Van Beeumen, J. J., Devreese, B. V., Van Bun, S. M., Hoff, W. D., Hellingwerf, K. J., Meyer, T. E., McRee, D. E., and Cusanovich, M. A. (1993) *Protein Sci. 2*, 1114−1125.
10. Borgstahl, G. E. O., Williams, D. R., and Getzoff, E. D. (1995) *Biochemistry 34*, 6278−6287.
11. Düx, P., Rubinstenn, G., Vuister, G. W., Boelens, R., Mulder, F. A. A., Hård, K., Hoff, W. D., Kroon, A. R., Crielaard, W., Hellingwerf, K. J., and Kaptein, R. (1998) *Biochem*istry *37*, 12689−12699.
12. Van Aalten, D. M. F., Crielaard, W., Hellingwerf, K. J., and Joshua-Tor, L. (2000) *Protein Sci. 9*, 64−72.
13. Pellequer, J. L., Wager-Smith, K. A., Kay, S. A., and Getzoff, E. D. (1998) *Proc. Natl. Acad. Sci. U.S.A. 95*, 5884−5890.
14. Devanathan, S., Genick, U. K. , Getzoff, E. D., Meyer, T. E., Cusanovich, M. A., and Tollin, G. (1997) *Arch. Biochem. Biophys. 340*, 83−89.
15. Lee, B. C., Croonquist, P. A., Sosnick, T. R., and Hoff, W. D. (2001) *J. Biol. Chem. 276*, 20821−20823.
16. Lee, B. C., Pandit, A., Croonquist, P. A., and Hoff, W. D. (2001) *PNAS 98*, 9062−9067.
17. Meyer, T. E., Devanathan, S., Woo, T. T., Getzoff, E. D., Tollin, G., and Cusanovich, M. A. (2003) *Biochemistry 42*, 3319−3325.
18. Meyer, T. E., Fitch, J. C., Bartsch, R. G., Tollin, G., and Cusanovich, M. A. (1990) *Biochim. Biophys. Acta 1016*, 364−370.
19. Koh, M., Van Driessche, G., Samyn, B., Hoff, W. D., Meyer, T. E., Cusanovich, M. A., and Van Beeumen, J. J. (1996) *Biochemistry 35*, 2526−2534.
20. Kort, R., Phillips-Jones, M. K., Van Aalten, D. M. F., Haker, A., Hoffer, S. M., Hellingwerf, K. J., and Crielaard, W. (1998) *Biochim. Biophys. Acta 1385*, 1−6.
21. Haker, A., Hendriks, J., Gensch, T., Hellingwerf, K., and Crielaard, W. (2000) *FEBS Lett. 486*, 52−56
22. Kyndt, J. A. (2003) Ph.D. Thesis, University of Gent, Gent, Belgium.
23. Jiang, Z. Y., Swem, L. R., Rushing, B. G., Devanathan, S., Tollin, G., and Bauer, C. E. (1999) *Science 285*, 406−409.
24. Sprenger, W. W., Hoff, W. D., Armitage, J. P., and Hellingwerf, K. J. (1993) *J. Bacteriol. 175*, 3096−3104.
25. Thiemann, B., and Imhoff, J. F. (1995) *Biochim. Biophys. Acta 1253*, 181−188.
26. Hoff, W. D., Sprenger, W. W., Postma, P. W., Meyer, T. E., Veenhuis, M., Leguijt, T., and Hellingwerf, K. J. (1994) *J. Bacteriol. 176*, 3920−3927.
27. Rajagopal, S., and Moffat, K. (2003) *Proc. Natl. Acad. Sci. U.S.A. 100*, 1649−1654.
28. Kyndt, J. A., Meyer, T. E., Cusanovich, M. A., and Van Beeumen, J. J. (2002) *FEBS Lett. 512*, 240−244.
29. Kyndt, J. A., Vanrobaeys, F., Fitch, J. C., Devreese, B. V., Meyer, T. E., Cusanovich, M. A., and Van Beeumen, J. J. (2003) *Biochemistry 42*, 965−970.
30. Gambetta, G. A., and Lagarias, J. C. (2001) *Proc. Natl. Acad. Sci. U.S.A. 98*, 10566−10571.
31. Bhoo, S. H., Davis, S. J., Walker, J., Karniol, B., and Vierstra, R. D. (2001) *Nature 414*, 776−779.
32. Meyer, T. E., Tollin, G., Hazzard, J. H., and Cusanovich, M. A. (1989) *Biophys. J. 56*, 559−564.
33. Imamoto, Y., Koshimizu, H., Mihara, K., Hisatomi, O., Mizukami, T., Tsujimoto, K., Kataoka, M., and Tokunaga, F. (2001) *Biochemistry 40*, 4679−4685.
34. Imamoto, Y., Kataoka, M., Tokunaga, F., Asahi, T., and Masuhara, H. (2001) *Biochemistry 40*, 6047−6052.
35. Brudler, R., Rammelsberg, R., Woo, T. T., Getzoff, E. D., and Gerwert, K. (2001) *Nature Struct. Biol. 8*, 265−270.
36. Xie, A., Kelemen, L., Hendriks, J., White, B. J., Hellingwerf, K. J., and Hoff, W. D. (2001) *Biochemistry 40*, 1510−1517.
37. Hoff, W. D., Van Stokkum, I. H. M., Van Ramesdonk, H. J., Van Brederode, M. E., Brouwer, A. M., Fitch, J. C., Meyer, T. E., Van Grondelle, R., and Hellingwerf, K. J. (1994) *Biochem. J. 67*, 1691−1705.
38. Borucki, B., Devanathan, S., Otto, H., Cusanovich, M. A., Tollin, G., and Heyn, M. P. (2002) *Biochemistry 41*, 10026−10037.
39. Ujj, L., Devanathan, S., Meyer, T. E., Cusanovich, M. A., Tollin, G., and Atkinson, G. H. (1998) *Biochem. J. 75*, 406−412.
40. Baltuska, A., Van Stokkum, I. H. M., Kroon, A., Monshouwer, R., Hellingwerf, K. H., and Van Grondelle, R. (1997) *Chem. Phys. Lett. 270*, 263−266.
41. Devanathan, S., Pacheco, A., Ujj, L., Cusanovich, M., Tollin, G., Lin, S., and Woodbury, N. (1999) *Biophys. J. 77*, 1017−1023.
42. Van Brederode, M. E., Gensch, T., Hoff, W. D., Hellingwerf, K. J., and Braslavsky, S. E. (1995) *Biophys. J. 68*, 1101−1109.
43. Meyer,T. E., Tollin, G., Causgrove, T. P., Cheng, P., and Blankenship, R. E. (1991) *Biochem. J. 59*, 988−991.
44. Hoff, W. D., Kwa, S. L. S., Van Grondelle, R., and Hellingwerf, K. J. (1992) *Photochem. Photobiol. 56*, 529−539.
45. Ng, K., Getzoff, E. D., and Moffat, K. (1995) *Biochemistry 34*, 879−890.
46. Imamoto, Y., Kataoka, M., and Tokunaga, F. (1996) *Biochemistry 35*, 14047−14053.
47. Van Brederode, M. E., Hoff, W. D., Van Stokkum, I. H. M., Groot, M. L., and Hellingwerf, K. J. (1996) *Biochem. J. 71*, 365−380.
48. Hoff, W. D., Xie, A., Van Stokkum, I. H. M., Tang, X. J., Gural, J., Kroon, A. R., and Hellingwerf, K. J. (1999) *Biochemistry 38*, 1009−1017.
49. Salamon, Z., Meyer, T. E., and Tollin, G. (1995) *Biophys. J. 68*, 648−654.
50. Brudler, R., Meyer, T. E., Genick, U. K., Devanathan, S., Woo, T. T., Millar, D. P., Gerwert, K., Cusanovich, M. A., Tollin, G., and Getzoff, E. D. (2000) *Biochemistry 39*, 13478−13486.
51. Genick, U. K., Devanathan, S., Meyer, T. E., Canestrelli, I. L., Williams, E., Cusanovich, M. A., Tollin, G., and Getzoff, E. D. (1997) *Biochemistry 36*, 8−14.
52. Demchuck, E., Genick, U. K., Woo, T. T., Getzoff, E. D., and Bashford, D. (2000) *Biochemistry 39*, 1100−1113.
53. Meyer, T. E., Cusanovich, M. A., and Tollin, G. (1993) *Arch. Biochem. Biophys. 306*, 515−517.
54. Hendriks, J., Hoff, W. D., Crielaard, W., and Hellingwerf, K. J. (1999) *J. Biol. Chem. 274*, 17655−17660.
55. Xie, A., Hoff, W. D., Kroon, A. R., and Hellingwerf, K. J. (1996) *Biochemistry 35*, 14671−14678.
56. Imamoto, Y., Mihara, K., Hisatomi, O., Kataoka, M., Tokunaga, F., Bojkova, N., and Yoshihara, K. (1997) *J. Biol. Chem. 272*, 12905−12908.
57. Genick, U., Gorgstahl, G. E. O, Ng, K., Ren, Z., Pradervand, C., Burke, P. M., Srajer, V., Teng, T. Y., Schildkamp, W., McRee, D. E., Moffat, K., and Getsoff, E. D. (1997) *Science 275*, 1471−1475.
58. Perman, B., Srajer, V., Ren, Z., Teng, T. Y., Pradervand, C., Ursby, T., Bourgeois, D., Schotte, F., Wulff, M., Kort, R., Hellingwerf, K. J., and Moffat, K. (1998) *Science 279*, 1946−1950.
59. Ren, Z., Perman, B., Srajer, V., Teng, T. Y., Pradervand, C., Bourgeois, D., Schotte, F., Ursby, T., Kort, R., Wulff, M., and Moffat, K. (2001) *Biochemistry 40*, 13788−13801.
60. Genick, U. K., Soltis, M., Kuhn, P., Canestrelli, I. L., and Getzoff, E. D. (1998) *Nature 392*, 206−209.
61. Heberle, J., and Gensch, T. (2001) *Nature Struct. Biol. 8*, 195−197.
62. Rubinstenn, G., Vuister, G. W., Mulder, F. A. A., Düx, P. E., Boelens, R., Hellingwerf, K. J., and Kaptein, R. (1998) *Nature Struct. Biol. 5*, 568−570.
63. Ohishi, S., Shimizu, N., Mihara, K., Imamoto, Y., and Kataoka, M. (2001) *Biochemistry 40*, 2854−2859.

64. Kandori, H., Iwata, T., Hendriks, J., Maeda, A., and Hellingwerf, K. J. (2000) *Biochemistry 39*, 7902−7909.
65. Mihara, K., Hisatomi, O., Imamoto, Y., Kataoka, M., and Tokunaga, F. (1997) *J. Biochem. 121*, 876−880.
66. Devanathan, S., Genick, U. K., Canestrelli, I. L., Meyer, T. E., Cuanovich, M. A., Getzoff, E. D., and Tollin, G. (1998) *Biochemistry 37*, 11563−11568.
67. Devanathan, S., Brudler, R., Hessling, B., Woo, T. T., Gerwert, K., Getzoff, E. D., Cusanovich, M. A., and Tollin, G. (1999) *Biochemistry 38*, 13766−13772.
68. Kumauchi, M., Hamada, N., Sasaki, J., and Tokunaga, F. (2002) *J. Biochem. 132*, 205−210.
69. Devanathan, S., Lin, S., Cusanovich, M. A., Woodbury, N., and Tollin, G. (2001) *Biophys. J. 81*, 2314−2319.
70. Devanathan, S., Lin, S., Cusanovich, M. A., Woodbury, N., and Tollin, G. (2000) *Biophys. J. 79*, 2132−2137.
71. Sasaki, J., Kumauchi, M., Hamada, N., Oka, T., and Tokunaga, F. (2002) *Biochemistry 41*, 1915−1922.
72. Miller, A., Leigeber, H., Hoff, W. D., and Hellingwerf, K. J. (1993) *Biochim. Biophys. Acta 1141*, 190−196.
73. Hendriks, J., Van Stokkum, I. H. M., Crielaard, W., and Hellingwerf, K. J. (1999) *FEBS Lett. 458*, 252−256.
74. Van Aalten, D. M. F., Haker, A., Hendriks, J., Hellingwerf, K. J., Joshua-Tor, L., and Crielaard, W. (2002) *J. Biol. Chem. 277*, 6463−6468.
75. Harigai, M., Yasuda, S., Imamoto, Y., Yoshihara, K., Tokunaga, F., and Kataoka, M. (2001) *J. Biochem. 130*, 51−56.
76. Van der Horst, M. A., Van Stokkum, I. H., Crielaard, W., and Hellingwerf, K. J. (2001) *FEBS Lett. 497*, 26−30.
77. Lagarias, D. M., Wu, S. H., and Lagarias, J. C. (1995) *Plant Mol. Biol. 29*, 1127−1142.
78. Ponting, C. P., and Aravind, L. (1997) *Curr. Biol. 7*, R674−677.
79. Gong, W., Hao, B., Mansy, S. S., Gonzalez, G., Gilles-Gonzalez, M. A., and Chan, M. K. (1998) *Proc. Natl. Acad. Sci. 95*, 15177−15182.
80. Gong, W., Hao, B., and Chan, M. K. (2000) *Biochemistry 39*, 3955−3962.
81. Miyatake, H., Kanai, M., Adachi, S., Nakamura, H., Tamura, K., Tanida, H., Tsuchiya, T., Iizuka, T., and Shiro, Y. (1999) *Acta Crystallogr. D55*, 1215−1218.
82. Morais Cabral, J. H., Lee, A., Cohen, S. L., Chait, B. T., Li, M., and Mackinnon, R. (1998) *Cell 95*, 649−655.
83. Ho, Y. S. J., Burden, L. M., and Hurley, J. H. (2000) *EMBO J. 19*, 5288−5299.
84. Crosson, S., and Moffat, K. (2001) *Proc. Natl. Acad. Sci. U.S.A. 98*, 2995−3000.
85. Vannini, A., Volpari, C., Gargioli, C., Muraglia, E., Cortese, R., De Francesco, R., Neddermann, P., and Di Marco, S. (2002) *EMBO J. 21*, 4393−4401.
86. Zhang, R., Pappas, T., Brace, J. L., Miller, P. C., Oulmassov, T., Molyneaux, J. M., Anderson, J. C., Bashkin, J. K., Winans, S. C., and Joachimiak, A. (2002) *Nature 417*, 971−974.
87. Gonzalez, L. C., Jr., Weis, W. I., and Scheller, R. H. (2001) *J. Biol. Chem. 276*, 24203−24211.
88. Martinez, S. E., Wu, A. Y., Glavas, N. A., Tang, Z. B., Turley, S., Hol, W. G. J., and Beavo, J. A. (2002) *Proc. Natl. Acad. Sci. U.S.A. 99*, 13260−13265.
89. Chik, J. K., Lindberg, U., and Schutt, C. E. (1996) *J. Mol. Biol. 263*, 607−623.
90. Procopio, M., Lahm, A., Tramontano, A., Bonati, L., and Pitea, D. (2002) *Eur. J. Biochem. 269*, 13−18.
91. Ohmori, M., Ikeuchi, M., Sato, N., Wolk, P., Kaneko, T., Ogawa, T., Kanehisa, M., Goto, S., Kawashima, S., Okamoto, S., Yoshimura, H., Katoh, H., Fujisawa, T., Ehira, S., Kamei, A., Yoshihara, S., Narikawa, R., and Tabata, S. (2001) *DNA Res. 8*, 271−284.
92. Galperin, M. Y., Nikolskaya, A. N., and Koonin, E. V. (2001) *FEMS Microbiol. Lett. 203*, 11−21.
93. Montgomery, B. L., and Lagarias, J. C. (2002) *Trends Plant Sci. 7*, 357−366.
94. Craven, C. J., Derix, N. M., Hendriks, J., Boelens, R., Hellingwerf, K. J., and Kaptein, R. (2000) *Biochemistry 39*, 14392−14399.

BI020690E